THE JOURNAL OF PHYSICAL CHEMISTRY A

pubs.acs.org/JPCA Article

Transition Metal Spin-State Energetics by MC-PDFT with High Local Exchange

Samuel J. Stoneburner, Donald G. Truhlar,* and Laura Gagliardi*

Cite This: J. Phys. Chem. A 2020, 124, 1187−1195 Read Online

ACCESS | Metrics & More | Article Recommendations | Supporting Information

ABSTRACT: The energetics of the spin states of transition metal complexes have been explored with a variety of electronic structure methods, but the calculations require a compromise between accuracy and affordability. In this work, the spin splittings of several iron complexes are studied with multiconfiguration pair-density functional theory (MC-PDFT). The results are compared to previously published results obtained by complete active space second-order perturbation theory (CASPT2) and CASPT2 with coupled-cluster semicore correlation (CASPT2/CC). In contrast to CASPT2's systematic overstabilization of high-spin states with respect to the CASPT2/CC reference, MC-PDFT with the tPBE on-top functional understabilizes high-spin states. This systematic understabilization is largely corrected by revising the exchange and correlation contributions to the on-top functional using the high local-exchange approximation (tPBE-HLE). Moreover, tPBE-HLE correctly predicts the spin of the ground state in most cases, while CASPT2 incorrectly predicts high-spin ground states in all cases. This is encouraging for practical work because tPBE and tPBE-HLE are faster than CASPT2 by a factor of 50 even in a moderately sized example.

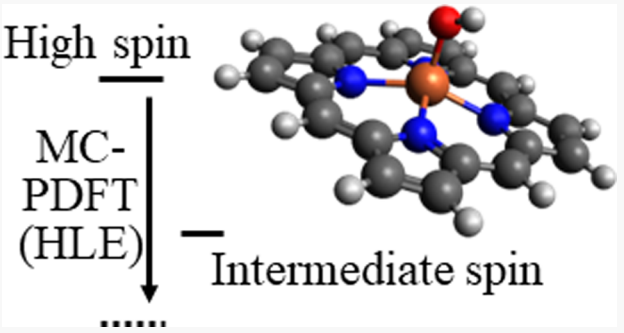

1. INTRODUCTION

Understanding the spin-state energetics of transition metal complexes is important for applications such as catalysis[1−3] and magnetic property investigations.[4,5] In this regard, iron complexes such as porphyrins have been extensively studied with theory[5−26] and are also often chosen as model systems for testing electronic structure methods,[14,24,25,27−40] in part due to an abundance of experimental results.[4,5,41−49]

The most widely used electronic structure method for studying this problem is Kohn−Sham density functional theory (KS-DFT),[50] which is often the only available high-level choice with an affordable cost.[51] However, the strong correlation of many transition metal complexes presents difficulties for KS-DFT, where "strong correlation" denotes the need to include more than one configuration in the electronic structure even for a good zero-order representation, where a configuration is a specific way of assigning electrons to orbitals. In particular, the Slater determinant of KS-DFT is not necessarily a spin eigenfunction, which is an issue that is sometimes called spin contamination.[28,52−54] Moreover, local exchange−correlation functionals are known to understabilize high-spin states,[55−60] which is due in part to overdelocalization[58−64] as well as spin contamination; however, some recent local functionals seem to be less afflicted with these deficiencies.[65,66] In the context of iron porphyrins, strong dependence of spin-state energetics on the choice of the exchange−correlation functional has been observed.[9−11,13−17] For example, Ghosh found that local exchange−correlation density functionals failed to properly describe the spin-state energetics and that the calculated spin densities vary widely among the tested functionals.[9] Pierloot and co-workers also found significant variation.[10,11,15]

Wave function theory (WFT) provides many options for cases where KS-DFT results are unreliable, but these options present other challenges. For reliable calculations on weakly correlated systems, the coupled-cluster method with singles, doubles, and quasiperturbative triples (CCSD(T))[67] is widely preferred; however, the common practice of using restricted-spin open-shell KS-DFT to generate input orbitals for restricted-spin CCSD(T) has recently been called into question.[68] More serious problems for treating transition metal complexes by CCSD(T), however, are cost and strong correlation. Radoń[17] provided CCSD(T) calculations for a variety of iron porhyrin model systems, including the undecorated porphyrin FeP, but due to computational cost, this method is primarily for small model systems. Several exchange−correlation functionals were also employed; Radoń then estimated spin splittings for larger systems by combining CCSD(T) energetics of a small model with an estimate of the difference between the full system and the model system. The estimate was based on a trend line obtained by KS-DFT

Received: November 18, 2019
Revised: January 4, 2020
Published: January 21, 2020

https://dx.doi.org/10.1021/acs.jpca.9b10772
J. Phys. Chem. A 2020, 124, 1187−1195

calculations for both systems.[17] The accuracy of the CCSD(T) methods is questionable for strongly correlated cases; several diagnostic measures have been applied to these systems to provide indications of when the results can be considered reliable.[17,34,37]

Strongly correlated systems can be treated more reliably by using methods with a multiconfiguration zero-order wave function that may be provided by multiconfigurational self-consistent field (MCSCF) methods such as complete active space self-consistent field theory (CASSCF).[69] In CASSCF, all correct-spin configuration state functions are included for a user-specified number of electrons n in a selected set of N active orbitals. Optionally one may also enforce spatial symmetry. For singlets with $n = N$, so that every active orbital occupied in the dominant configuration has a correlating orbital; the current practical limit on the active space size that can be treated with conventional configuration interaction solvers is 18 electrons in 18 orbitals, or $(n,N) = (18,18)$.[70] Larger CASSCF active spaces are possible with other solvers, for example as large as (40,38)[39] with quantum Monte Carlo CASSCF (FCIQMC-CASSCF, also referred to as Stochastic-CASSCF)[32] or as large as (84,84)[71] with density matrix renormalization group (DMRG).[72−76] Another way to treat a larger number of active orbitals is the restricted active space self-consistent field (RASSCF)[77] method, in which one includes only a subset of the active space CSFs, or with RASCI,[78] where the orbitals are optimized with fewer CSFs than are used in the final configuration interaction step.

MCSCF methods include only a small portion of the dynamic correlation[79] and are not quantitatively accurate on their own, but rather, they serve as zero-order wave functions for post-SCF steps to obtain better energies. The correlation energy not contained in a CASSCF calculation is called the external correlation energy, and one widely employed post-SCF method is the second-order perturbation theory, as in CASPT2,[80−82] MRMP2,[83] RASPT2,[84] and DMRG-CASPT2,[85] which includes an external correlation by perturbatively adding single and double excitations. A disadvantage of these methods is their high computational cost[86,87] (in terms of both computer time and memory), and it has been observed that CASPT2 overstabilizes high-spin states by as much as 10 kcal/mol for first-row transition metal complexes.[34,60] Pierloot et al. studied this systematic error in first-row transition metal complexes and concluded that it is due to the inconsistent treatment of semicore correlation (sometimes called subvalence correlation,[88−90] which in the present case is correlation associated with excitations from 3s and 3p orbitals).[34] Phung et al.[37] (henceforth denoted PHFP) then proposed a combined CASPT2/CC method featuring CASPT2 for the valence correlation and CCSD(T) or CCSD[91] for the semicore correlation and concluded that the high-spin overstabilization, while not completely eliminated, was reduced to about 2 kcal/mol. The authors also noted that the application of CASPT2/CC is expected to be restricted to weakly correlated cases.[37] A recent study by Radoń on a different set of iron systems again concluded that CASPT2/CC reduces the error in CASPT2.[92]

An economical alternative to CASPT2 is multiconfiguration pair-density functional theory (MC-PDFT),[93,94] which takes the electron density and pair density from a preceding MCSCF calculation and applies an on-top functional analogous to the exchange-correlation functional of KS-DFT. Because the MCSCF wave function is a spin eigenfunction, spin contamination is completely avoided.[95] Furthermore, MC-PDFT automatically includes semicore correlation (and even core correlation, to the extent allowed by the basis set). MC-PDFT has been used with CASSCF, RASSCF, RASCI, and CASSCF-DMRG wave functions in applications to a variety of transition metal complexes,[64,86,87,96−102] including unmodified iron porphyrin (FeP).[40]

The first generation of on-top functionals are translations of KS-DFT functionals, e.g., tPBE[93] from PBE.[103] Recently in KS-DFT, more accurate band gaps and molecular Rydberg excitations were obtained by multiplying the exchange contribution by a factor of 1.25 and the correlation by a factor of 0.5 (labeled "high local exchange" or HLE[65,66]). In the context of MC-PDFT, Sharma et al.[104] found that translating the PBE functional with HLE, yielding an on-top functional called tPBE-HLE, improved the calculated excitation energies of benzene, but Presti et al.[105] found that tPBE-HLE offered at best slight improvement in calculated excitation energies when tested more broadly. One may conclude that HLE is not a prescription for universal improvement in either KS-DFT or MC-PDFT, but it may have advantages and practical usefulness for certain types of applications. In the present work, we examine the performance of tPBE and tPBE-HLE for spin-changing excitation energies of iron complexes.

As our calculations are for electronic energies without including vibrational contributions, they cannot be compared directly to experiments (and, anyway, the experimental numbers are often unavailable or uncertain). In light of the demonstrated high-spin overstabilization of CASPT2 for transition metal excitation energies, we choose to use the CASPT2/CC values of PHFP as the best available "benchmark"; however, we should keep in mind the possible unreliability of the CC correction for strongly correlated systems. With this choice of benchmark, our target molecules (Figure 1) consist of unsubstituted iron porphyrins (FeP), iron porphyrins substituted with additional ligands (FePXH and $FeP(NH_3)OH$), and their respective small model compounds with two amidine ligands (FeL_2, FeL_2XH, and Fe $L_2(NH_3)$-OH)). A model of a synthetic nonheme oxidant, $[Fe(NH_3)_5O]^{2+}$,[106,107] is also included.

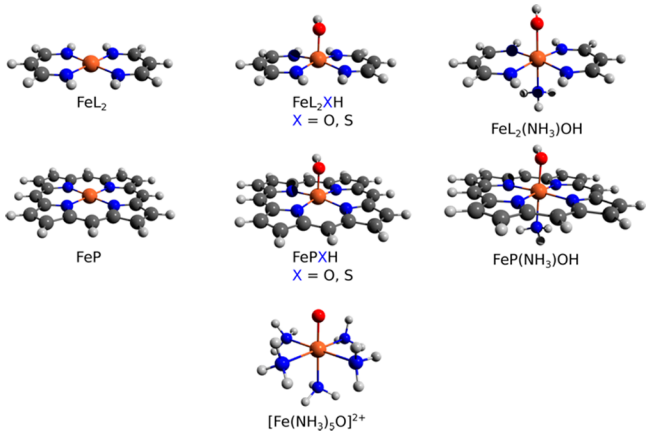

Figure 1. Iron complexes considered in this work. Reprinted with permission from ref 37. Copyright 2018 American Chemical Society.

https://dx.doi.org/10.1021/acs.jpca.9b10772
J. Phys. Chem. A 2020, 124, 1187−1195

Table 1. ΔE and Mean Unsigned Deviations (MUDs) from PT2/CC (kcal/mol)

complex	HS term (n,N)[a]	term	tPBE	tPBE-HLE	trevPBE	trevPBE-HLE	CASPT2[37]	CASPT2/CC[37]
FeL_2	^5A_g	^1A_g	14.25	24.83	15.41	26.28	37.84	31.92
	(8,11/10)	$^3B_{1g}$	−13.46	0.51	−10.44	4.27	−2.28	−4.80
		$^3B_{3g}$	−16.67	−4.04	−13.49	−0.07	−4.63	−6.83
FeL_2OH	$^6A'$	$^2A''$	−17.59	0.98	−13.64	5.92	10.25	6.55
	(11,15/13)	$^4A''$	−13.03	−0.23	−10.07	3.47	6.90	4.68
FeL_2SH	$^6A'$	$^2A''$	−29.86	−15.95	−25.01	−9.90	−9.21	−11.61
	(11,13/11)	$^4A''$	−17.26	−5.64	−14.26	−1.89	0.31	−1.78
$FeL_2(NH_3)OH$	$^6A'$	$^2A''$	−31.09	−10.94	−26.26	−4.91	−4.63	−8.58
	(11,15/13)	$^4A''$	−6.95	5.42	−3.89	9.25	12.12	9.69
FeP	$^5A_{1g}$	$^1A_{1g}$	15.31	23.84	15.82	24.49	38.03	32.41
	(8,11)	$^3A_{2g}$	−8.43	1.09	−6.57	3.42	3.74	0.34
		^3E_g	−7.28	0.25	−5.56	2.40	5.65	2.29
FePOH	$^6A'$	$^2A''$	−9.25	5.67	−6.63	8.94	18.81	14.27
	(11,15/13)	$^4A''$	−8.20	3.34	−6.06	6.02	12.40	9.85
FePSH	$^6A'$	$^2A''$	−16.41	−7.85	−12.88	−3.43	2.13	−1.03
	(11,13/11)	$^4A''$	−11.13	−1.81	−8.85	1.03	6.53	4.05
$FeP(NH_3)OH$	$^6A'$	$^2A''$	−28.73	−12.32	−26.09	−9.02	1.31	−3.59
	(11,15/13)	$^4A''$	−6.50	4.69	−4.89	6.71	14.88	11.88
$[Fe(NH_3)_5O]^{2+}$	$^5A'$	$^3A''$	−9.97	−1.23	−7.00	2.49	2.50	−0.42
	(12,16/15)							
MUD, low- and intermediate-spin			16.3	5.0	13.6	3.7	4.2	
MUD, low-spin only			20.5	6.5	17.5	4.1	6.0	
MUD, intermediate-spin only			13.3	3.9	10.8	3.4	3.0	

[a]Active spaces were smaller for the low-spin states except for FeP. See also Tables S5−S7.

2. COMPUTATIONAL METHODS

We used MC-PDFT[93] with several on-top functionals, namely tPBE[93] translated from PBE,[103] trevPBE[108] translated from revPBE,[109] tBLYP[93] translated from BLYP,[110,111] and tPBE-HLE[104] translated from PBE-HLE.[104]

Spin-splittings (ΔE) are defined as

$$\Delta E = E_{IS,LS} - E_{HS} \quad (1)$$

where IS and LS indicate either intermediate spin and low spin, respectively, HS indicates high spin, and E is the energy. Note that a negative ΔE value indicates the intermediate or low spin is favored.

The CASPT2[80,81] and CASPT2/CC results from PHFP include both the valence and semicore correlation energy (these results are labeled ΔE(+sp) in refs 34 and 37). Additional CASPT2 calculations were performed in the present work in order to facilitate timing comparisons with MC-PDFT. All CASPT2 calculations had the default ionization potential electron affinity (IPEA) shift[112] of 0.25 au, designed to correct systematic errors, and an imaginary shift[113] of 0.1 au to reduce problems with intruder states; these options are the same as in PHFP. However, while PHFP used Molcas 8.1,[70] we used Molcas 8.2[70] because of its more complete implementation of MC-PDFT.

Input and orbital files were obtained from the authors of PHFP to ensure the same orbitals would be used for the CASSCF,[114] CASPT2, and MC-PDFT calculations in the present work. The active spaces for all systems other than $[Fe(NH_3)_5O]^{2+}$ were the same as those selected in ref 34 and include all 3d and 3d′ orbitals of the Fe plus ligand orbitals judged to have important covalent interactions with the 3d orbitals of Fe. For some low-spin states, the 3d′ orbitals corresponding to unoccupied 3d orbitals were omitted from the active space to prevent mixing or rotation into other virtual orbitals. The active spaces for $[Fe(NH_3)_5O]^{2+}$ are the same as those in PHFP, where the 3d′ orbitals are included in the active space only for occupied 3d orbitals.

In PHFP, a variety of correlation consistent (cc) basis sets were used in order to extrapolate to the complete basis set (CBS) limit. In order to minimize questions of basis set dependency, our calculations used awC5Z/aTZ, which is the basis set found to be closest to the CBS limit; awC5Z/aTZ is a shorthand notation used in PHFP for aug-cc-pwCV5Z-DK[115] on Fe, cc-pVTZ-DK on H, and aug-cc-pVTZ- DK[116−118] on all other atoms, where wCV denotes weighted core−valence and means that the basis functions capable of treating both valence and core−valence correlation are included (without core−core correlation), aug means that the basis set is augmented with diffuse functions to describe weak interactions, and DK means that the basis sets are designed for use with the Douglas−Kroll−Hess treatment of scalar relativistic effects. Cholesky decomposition[119] was used with a threshold of 10^{-6} au to reduce the memory and storage requirements of the two-electron integrals. A second-order Douglas−Kroll−Hess Hamiltonian[120−122] was employed to account for scalar relativity. The CASPT2/CC results from PHFP presented throughout this work are taken from Table 3 (their CCSD(T) Δ_{sp}) and from Tables S2 and S5−S9 in the Supporting Information (their CASPT2 ΔE(*no*sp) and Δ_{sp} using awC5z/aTZ).

Results for tBLYP are reported in Table S1. Results for tPBE, tPBE-HLE, trevPBE, and trevPBE-HLE are reported below.

3. RESULTS AND DISCUSSION

Our primary results are presented in Table 1, where the HS states are quintets or sextets, the IS states are triplets or

https://dx.doi.org/10.1021/acs.jpca.9b10772
J. Phys. Chem. A 2020, 124, 1187−1195

Table 2. Ground States of Complexes. For Convenience, Correct Predictions are Bold

system	$(n,N)^a$	experimental[b]	tPBE	tPBE-HLE	CASPT2[37],[b]	CASPT2/CC[37],[b]
FeP	(8,11)	triplet[d]	**triplet**	quintet	quintet	quintet
FePSH	(11,11/13)	doublet[e]	**doublet**	**doublet**	sextet	**doublet**
$FeP(NH_3)OH$	(11,11/13)	doublet[f]	**doublet**	**doublet**	sextet	**doublet**
$[Fe(NH_3)_5O]^{2+}$	(12,15/16)	triplet[g]	**triplet**	**triplet**	quintet	**triplet**

[a]Active spaces were smaller for the low-spin states except for FeP. See also Tables S5−S7. [b]Experimental work was conducted on more complicated systems, of which the systems studied here can be understood as models. For more detail see PHFP. [c]While CASPT2/CC incorrectly predicts a high-spin ground state for FeP with the awC5Z/aTZ basis set, it correctly predicts all of the experimental ground spin states in the CBS-extrapolated results presented in Table 3 of PHFP. In contrast, the entirely incorrect CASPT2 awC5Z/aTZ predictions shown here are unchanged from the CASPT2 CBS results of PHFP. [d]Refs 41, 42, and 46. [e]Ref 43. [f]Refs 49 and 123. [g]Ref 124.

quartets, and the LS states are singlets or doublets. The CASPT2 and CASPT2/CC results are from PHFP and we use CASPT2/CC as our benchmark.

Table 1 shows that the CASPT2 results are consistently more positive or less negative than CASPT2/CC, as discussed in ref 34 and PHFP. In contrast, tPBE and trevPBE results are consistently more negative or less positive than CASPT2/CC, similar to the high-spin understabilization that is expected in KS-DFT with a local exchange−correlation functional like PBE. Furthermore, the mean unsigned deviations (MUDs) of tPBE and trevPBE from the benchmark are much larger than for CASPT2 (16.3 and 13.6 vs 4.2 kcal/mol, respectively). However, MC-PDFT with tPBE-HLE and trevPBE-HLE performs much better than KS-DFT with PBE and better than MC-PDFT with tPBE and trevPBE; tPBE-HLE and trevPBE-HLE have MUDs of only 5.0 and 3.7 kcal/mol, respectively. The MUD for trevPBE-HLE is particularly noteworthy for being smaller than the 4.2 kcal/mol MUD of CASPT2. The individual unsigned deviations for tPBE-HLE and trevPBE-HLE are all smaller than for their respective unmodified functionals, usually by at least a factor of 2. With only a few exceptions, the tPBE-HLE and trevPBE-HLE deviations are negative, indicating that for the most part the adjustments to the exchange and correlation do not over-compensate for the high-spin understabilization in tPBE and trevPBE. The negative deviations are also encouraging in light of PFHP's comment that CASPT2/CC likely overestimates the stability of high-spin states by about 2 kcal/mol, implying that the true spin splittings may be slightly more negative than the CASPT2/CC reference, and hence, the error in the tPBE-HLE and trevPBE calculations may be even smaller than the MUD in the table.

The systematic nature of the deviations in Table 1 is more manifest when we examine LS−HS versus IS−HS splittings separately. The deviations for IS−HS splittings are almost always of a smaller magnitude than the LS−HS deviations for the same system. The trend does not depend on whether the LS−HS case or the IS−HS case(s) have larger magnitudes in the CASPT2/CC reference values.

An analysis of the differences in the absolute energies between tPBE and tPBE-HLE shows that HLE accomplishes its correction of tPBE's high-spin understabilization primarily by changing the calculated energy of the high-spin state, for which the energy is always decreased by 7−20 kcal/mol more than the low-spin states (specific values are presented in section S4). The same trend holds for trevPBE and trevPBE-HLE.

We also note that tBLYP-HLE yields the same good MUD of 5.1 kcal/mol as tPBE-HLE. See Table S1 for more details.

3.1. Ground Spin States. PHFP discussed some cases for which their CBS-extrapolated CASPT2 and CASPT2/CC results disagreed regarding the ground state compared to experimental ground states. We make some similar comparisons in Table 2. Note that the experimental ground states were determined for larger systems than these model complexes and that neither our work nor the work in PHFP accounts for factors such as vibrational corrections or solvent effects. The agreement with experiments for the ground spin states is quite better for both tPBE and TPBE-HLE than for CASPT2. Note that CASPT2 erroneously predicts a high-spin ground state in all four cases, while tPBE and tPBE-HLE correctly identify the low- or intermediate-spin (as appropriate) states as the ground state with the exception of tPBE-HLE with FeP.

3.2. Active Space Dependency for FeP. In the present work we have constrained ourselves to using the active spaces used by PHFP to enable a direct comparison with the CASPT2/CC reference values. However, the effect of active space selection for FeP has been noted on multiple occasions (e.g., refs 34, 39, and 40) and deserves some comment here.

CASPT2 incorrectly predicts the quintet $^5A_{1g}$ state to be below the triplet ^3E_g and $^3A_{2g}$ states in energy with both (8,11) and (16,15) active spaces.[34] However, Li Manni et al. recently demonstrated with stochastic-CASSCF that the ordering of the ^3E_g and $^5A_{1g}$ states can be corrected with an active space of (32,34) or (40,38), even with no post-MCSCF step.[39] To the best of our knowledge, CASPT2 has not yet been attempted with active spaces that large; RASPT2 with a (34,35) active space was reported in ref 27, but some of these same authors noted in ref 34 that there was a basis set error that significantly affected the results. However, Zhou et al. tested tPBE with a variety of active spaces and found that tPBE triplet−quintet gaps (with both triplet states) retained the same signs and varied by less than 2.2 kcal/mol between CASSCF-(8,11) and DMRG-CASSCF-(34,35),[40] demonstrating that MC-PDFT is quite stable in regard to active space selection for FeP. Additionally, their (8,11) results are within 0.15 kcal/mol of the tPBE results presented here, despite the different basis sets used. Given that HLE involves only a rescaling of the exchange and correlation, it is expected that the stability in regard to the active space would apply to tPBE-HLE as well. We tested this hypothesis by applying the HLE adjustments to the tPBE calculations from Zhou et al.[40] and confirmed that the stability with regard to the active space observed for tPBE carries forward to tPBE-HLE (see section S2 for more detail).

3.3. Timing Comparisons. One of the primary advantages of MC-PDFT over second-order perturbation theory is that it can be performed at a much lower computational cost, as shown in Table 3, where the costs correspond to computa-

https://dx.doi.org/10.1021/acs.jpca.9b10772
J. Phys. Chem. A 2020, 124, 1187−1195

Table 3. Comparison of Serial Computational Time for CASPT2 and MC-PDFT (h:min), Sorted by Sum of the Last Three Columns

						post-SCF	
system	(*n*,*N*)	state	BFs[a]	CSFs[b]	CASSCF[c]	CASPT2	MC-PDFT[d]
FeL_2[e]	(8,11)	^5A_g	860	5476	0:39	0:18	0:02
FeL_2	(8,10)	^1A_g	860	3540	0:41	0:17	0:02
FeL_2	(8,11)	$^3B_{1g}$	860	12720	0:42	0:19	0:02
FeL_2	(8,11)	$^3B_{3g}$	860	12740	0:50	0:17	0:02
FeP[f]	(8,11)	$^5A_{1g}$	1532	5476	3:32	3:18	0:10
FeL_2SH	(11,11)	$^2A''$	924	52272	4:22	2:31	0:16
FeP	(8,11)	$^1A_{1g}$	1532	8290	3:40	3:30	0:11
FeL_2SH	(11,13)	$^6A'$	924	156156	4:23	2:53	0:16
FeP	(8,11)	^3E_g	1532	12740	3:40	3:46	0:11
FeP	(8,11)	$^3A_{2g}$	1532	12720	3:45	3:46	0:11
FeL_2SH	(11,13)	$^4A''$	924	429534	4:27	3:09	0:16
FeL_2OH	(11,13)	$^2A''$	920	490776	4:30	3:17	0:16
$[Fe(NH_3)_5O]^{2+}$	(12,15)	$^3A''$	746	5271210	3:44	4:23	0:10
FeL_2OH	(11,15)	$^4A''$	920	2928170	4:42	5:10	0:17
$[Fe(NH_3)_5O]^{2+}$	(12,16)	$^5A'$	746	8509200	2:59	8:03	0:09

[a]Number of contracted basis functions. [b]Number of configuration state functions. [c]The time for CASSCF includes the time for calculating the one- and two-electron integrals. [d]This time is the same for tPBE and tPBE-HLE. [e]L denotes an amidine ligand, as explained in the Introduction. See Figure 1. [f]P denotes porphyrin, as explained in the Introduction. See Figure 1.

tional time requirements for serial calculations on Haswell E5-2680v3 processors. Note that as the CASPT2 calculation time increases, it eventually becomes larger than the CASSCF step, which is dominated by the integral evaluation time for the calculations in this table because of the large basis sets. In the most extreme case shown, which is the last row of Table 3, CASPT2 takes over 70% of the combined time for CASSCF and CASPT2, whereas the tPBE step requires only 5% of the time of the CASSCF step; therefore, the MC-PDFT post-SCF step is faster than the CASPT2 post-SCF step by a factor of 50. Several larger calculations are not shown in Table 3 because they were run only in parallel. Our previous work on organic diradicals[95] leads us to expect the relative cost benefit of MC-PDFT over CASPT2 to be greater for these larger calculations. The MC-PDFT calculations also require less memory.

4. CONCLUSIONS

While CASPT2 demonstrates a consistent overstabilization of high-spin states and the tPBE on-top functional demonstrates an even stronger systematic understabilization of high-spin states, tPBE with high local exchange (tPBE-HLE) yields deviations from CASPT2/CC reference values that are only slightly larger than CASPT2 (5.0 vs 4.2 kcal/mol, respectively), and trevPBE-HLE yields deviations that are smaller than CASPT2 (3.7 vs 4.2 kcal/mol, respectively). Furthermore, tPBE-HLE correctly identifies most of the ground states inferred from the experiments on smaller models, while CASPT2 incorrectly predicts high-spin ground states in all cases. Similar improvements were observed with other MC-PDFT functionals, and future functional development may yield additional advantages. Further comparisons with CASPT2/CC will require a more diverse test set and a better understanding of the limits of the CASPT2/CC method, but the results in this work show that HLE significantly improves MC-PDFT's description of spin-state energetics in iron complexes.

MC-PDFT provides significant cost advantages over CASPT2 as well. The systems in this study were treated with small active spaces, but for systems requiring larger active spaces, the cost considerations will be determinative in the choice of methods, and the computational-cost advantages of MC-PDFT will be critical. Moreover, the recent development of DMRG-PDFT[125] enables the use of tPBE-HLE (or tPBE) even for very large active spaces, which may be necessary, for example, for treating systems with multiple transition metal centers.

■ ASSOCIATED CONTENT

Supporting Information

The Supporting Information is available free of charge at https://pubs.acs.org/doi/10.1021/acs.jpca.9b10772.

Δ*E* results for tBLYP, with and without HLE. tPBE-HLE results for FeP with the active spaces of ref 40. MC-PDFT absolute energies. Relative changes in energy in comparing tPBE to tPBE-HLE. M-diagnostic results. (PDF)

■ AUTHOR INFORMATION

Corresponding Authors

Donald G. Truhlar − *Department of Chemistry, Chemical Theory Center, and Minnesota Supercomputing Institute, University of Minnesota, Minneapolis, Minnesota 55455-0431, United States;* orcid.org/0000-0002-7742-7294; Email: truhlar@umn.edu

Laura Gagliardi − *Department of Chemistry, Chemical Theory Center, and Minnesota Supercomputing Institute, University of Minnesota, Minneapolis, Minnesota 55455-0431, United States;* orcid.org/0000-0001-5227-1396; Email: gagliard@umn.edu

Author

Samuel J. Stoneburner − *Department of Chemistry, Chemical Theory Center, and Minnesota Supercomputing Institute, University of Minnesota, Minneapolis, Minnesota 55455-0431, United States;* orcid.org/0000-0001-8394-0572

https://dx.doi.org/10.1021/acs.jpca.9b10772
J. Phys. Chem. A 2020, 124, 1187−1195

Complete contact information is available at:
https://pubs.acs.org/10.1021/acs.jpca.9b10772

Notes

The authors declare no competing financial interest.

■ ACKNOWLEDGMENTS

The authors thank Kristine Pierloot for providing files associated with PHFP and Chen Zhou for providing files associated with ref 40. The authors also thank Larry Que for helpful conversations. This work was supported in part by the National Science Foundation under Grant No. CHE-1746186.

■ REFERENCES

(1) Harvey, J. N.; Poli, R.; Smith, K. M. Understanding the Reactivity of Transition Metal Complexes Involving Multiple Spin States. *Coord. Chem. Rev.* **2003**, *238*−*239*, 347−361.
(2) Meunier, B.; de Visser, S. P.; Shaik, S. Mechanism of Oxidation Reactions Catalyzed by Cytochrome P450 Enzymes. *Chem. Rev.* **2004**, *104*, 3947−3980.
(3) Bauer, I.; Knölker, H.-J. Iron Catalysis in Organic Synthesis. *Chem. Rev.* **2015**, *115*, 3170−3387.
(4) Goff, H.; La Mar, G. N.; Reed, C. A. Nuclear Magnetic Resonance Investigation of Magnetic and Electronic Properties of "Intermediate Spin" Ferrous Porphyrin Complexes. *J. Am. Chem. Soc.* **1977**, *99*, 3641−3646.
(5) Stavretis, S. E.; Atanasov, M.; Podlesnyak, A. A.; Hunter, S. C.; Neese, F.; Xue, Z. L. Magnetic Transitions in Iron Porphyrin Halides by Inelastic Neutron Scattering and Ab Initio Studies of Zero-Field Splittings. *Inorg. Chem.* **2015**, *54*, 9790−9801.
(6) Liao, M. S.; Scheiner, S. Electronic Structure and Bonding in Metal Porphyrins, Metal = Fe, Co, Ni, Cu, Zn. *J. Chem. Phys.* **2002**, *117*, 205−219.
(7) Schöneboom, J. C.; Lin, H.; Reuter, N.; Thiel, W.; Cohen, S.; Ogliaro, F.; Shaik, S. The Elusive Oxidant Species of Cytochrome P450 Enzymes: Characterization by Combined Quantum Mechanical/Molecular Mechanical (QM/MM) Calculations. *J. Am. Chem. Soc.* **2002**, *124*, 8142−8151.
(8) Groenhof, A. R.; Swart, M.; Ehlers, A. W.; Lammertsma, K. Electronic Ground States of Iron Porphyrin and of the First Species in the Catalytic Reaction Cycle of Cytochrome P450s. *J. Phys. Chem. A* **2005**, *109*, 3411−3417.
(9) Ghosh, A. Transition Metal Spin State Energetics and Noninnocent Systems: Challenges for DFT in the Bioinorganic Arena. *JBIC, J. Biol. Inorg. Chem.* **2006**, *11*, 712−724.
(10) Pierloot, K.; Vancoillie, S. Relative Energy of the High-($^5T_{2g}$) and Low-($^1A_{1g}$) Spin States of the Ferrous Complexes [Fe(L)-(NHS_4)]: CASPT2 versus Density Functional Theory. *J. Chem. Phys.* **2008**, *128*, No. 034104.
(11) Radoń, M.; Pierloot, K. Binding of CO, NO, and O_2 to Heme by Density Functional and Multireference Ab Initio Calculations. *J. Phys. Chem. A* **2008**, *112*, 11824−11832.
(12) Cramer, C. J.; Truhlar, D. G. Density Functional Theory for Transition Metals and Transition Metal Chemistry. *Phys. Chem. Chem. Phys.* **2009**, *11*, 10757−10816.
(13) Vancoillie, S.; Zhao, H.; Radoń, M.; Pierloot, K. Performance of CASPT2 and DFT for Relative Spin-State Energetics of Heme Models. *J. Chem. Theory Comput.* **2010**, *6*, 576−582.
(14) Radoń, M.; Broclawik, E.; Pierloot, K. DFT and Ab Initio Study of Iron-Oxo Porphyrins: May They Have a Low-Lying Iron(V)-Oxo Electromer? *J. Chem. Theory Comput.* **2011**, *7*, 898−908.
(15) Radoń, M.; Pierloot, K. Correction to "Binding of CO, NO, and O_2 to Heme by Density Functional and Multireference Ab Initio Calculations". *J. Phys. Chem. A* **2011**, *115*, 7871−7871.
(16) Ali, M. E.; Sanyal, B.; Oppeneer, P. M. Electronic Structure, Spin-States, and Spin-Crossover Reaction of Heme-Related Fe-Porphyrins: A Theoretical Perspective. *J. Phys. Chem. B* **2012**, *116*, 5849−5859.
(17) Radoń, M. Spin-State Energetics of Heme-Related Models from DFT and Coupled Cluster Calculations. *J. Chem. Theory Comput.* **2014**, *10*, 2306−2321.
(18) Gani, T. Z. H.; Kulik, H. J. Unifying Exchange Sensitivity in Transition-Metal Spin-State Ordering and Catalysis through Bond Valence Metrics. *J. Chem. Theory Comput.* **2017**, *13*, 5443−5457.
(19) Kupper, C.; Mondal, B.; Serrano-Plana, J.; Klawitter, I.; Neese, F.; Costas, M.; Ye, S.; Meyer, F. Nonclassical Single-State Reactivity of an Oxo-Iron(IV) Complex Confined to Triplet Pathways. *J. Am. Chem. Soc.* **2017**, *139*, 8939−8949.
(20) Gutsev, G. L.; Bozhenko, K. V.; Gutsev, L. G.; Utenyshev, A. N.; Aldoshin, S. M. Dependence of Properties and Exchange Coupling Constants on the Charge in the Mn_2O_n and Fe_2O_n Series. *J. Phys. Chem. A* **2018**, *122*, 5644−5655.
(21) Li Manni, G.; Alavi, A. Understanding the Mechanism Stabilizing Intermediate Spin States in Fe(II)-Porphyrin. *J. Phys. Chem. A* **2018**, *122*, 4935−4947.
(22) Nachtigallová, D.; Antalík, A.; Lo, R.; Sedlák, R.; Manna, D.; Tuček, J.; Ugolotti, J.; Veis, L.; Legeza, Ö.; Pittner, J.; et al. An Isolated Molecule of Iron(II) Phthalocyanin Exhibits Quintet Ground-State: A Nexus between Theory and Experiment. *Chem. - Eur. J.* **2018**, *24*, 13413−13417.
(23) Phung, Q. M.; Pierloot, K. The Dioxygen Adducts of Iron and Manganese Porphyrins: Electronic Structure and Binding Energy. *Phys. Chem. Chem. Phys.* **2018**, *20*, 17009−17019.
(24) Pinter, B.; Al-Saadon, R.; Chen, Z.; Yang, W. Spin-State Energetics of Iron(II) Porphyrin from the Particle-Particle Random Phase Approximation. *Eur. Phys. J. B* **2018**, *91*, 270.
(25) Guo, M.; Källman, E.; Pinjari, R. V.; Couto, R. C.; Kragh Sørensen, L.; Lindh, R.; Pierloot, K.; Lundberg, M. Fingerprinting Electronic Structure of Heme Iron by Ab Initio Modeling of Metal L-Edge X-Ray Absorption Spectra. *J. Chem. Theory Comput.* **2019**, *15*, 477−489.
(26) Phung, Q. M.; Pierloot, K. Low-Lying Electromeric States in Chloro-Ligated Iron(IV)-Oxo Porphyrin as a Model for Compound I, Studied with Second-Order Perturbation Theory Based on Density Matrix Renormalization Group. *J. Chem. Theory Comput.* **2019**, *15*, 3033−3043.
(27) Vancoillie, S.; Zhao, H.; Tran, V. T.; Hendrickx, M. F. A.; Pierloot, K. Multiconfigurational Second-Order Perturbation Theory Restricted Active Space (RASPT2) Studies on Mononuclear First-Row Transition-Metal Systems. *J. Chem. Theory Comput.* **2011**, *7*, 3961−3977.
(28) Luo, S.; Truhlar, D. G. How Evenly Can Approximate Density Functionals Treat the Different Multiplicities and Ionization States of 4d Transition Metal Atoms? *J. Chem. Theory Comput.* **2012**, *8*, 4112−4126.
(29) Maurice, R.; Verma, P.; Zadrozny, J. M.; Luo, S.; Borycz, J.; Long, J. R.; Truhlar, D. G.; Gagliardi, L. Single-Ion Magnetic Anisotropy and Isotropic Magnetic Couplings in the Metal-Organic Framework Fe_2(dobdc). *Inorg. Chem.* **2013**, *52*, 9379−9389.
(30) Luo, S.; Averkiev, B.; Yang, K. R.; Xu, X.; Truhlar, D. G. Density Functional Theory of Open-Shell Systems. The 3d-Series Transition-Metal Atoms and Their Cations. *J. Chem. Theory Comput.* **2014**, *10*, 102−121.
(31) Saitow, M.; Kurashige, Y.; Yanai, T. Fully Internally Contracted Multireference Configuration Interaction Theory Using Density Matrix Renormalization Group: A Reduced-Scaling Implementation Derived by Computer-Aided Tensor Factorization. *J. Chem. Theory Comput.* **2015**, *11*, 5120−5131.
(32) Li Manni, G.; Smart, S. D.; Alavi, A. Combining the Complete Active Space Self-Consistent Field Method and the Full Configuration Interaction Quantum Monte Carlo within a Super-CI Framework, with Application to Challenging Metal-Porphyrins. *J. Chem. Theory Comput.* **2016**, *12*, 1245−1258.
(33) Phung, Q. M.; Wouters, S.; Pierloot, K. Cumulant Approximated Second-Order Perturbation Theory Based on the

Density Matrix Renormalization Group for Transition Metal Complexes: A Benchmark Study. *J. Chem. Theory Comput.* **2016**, *12*, 4352−4361.
(34) Pierloot, K.; Phung, Q. M.; Domingo, A. Spin State Energetics in First-Row Transition Metal Complexes: Contribution of (3s3p) Correlation and Its Description by Second-Order Perturbation Theory. *J. Chem. Theory Comput.* **2017**, *13*, 537−553.
(35) Smith, J. E. T.; Mussard, B.; Holmes, A. A.; Sharma, S. Cheap and Near Exact CASSCF with Large Active Spaces. *J. Chem. Theory Comput.* **2017**, *13*, 5468−5478.
(36) Verma, P.; Varga, Z.; Klein, J. E. M. N.; Cramer, C. J.; Que, L.; Truhlar, D. G. Assessment of Electronic Structure Methods for the Determination of the Ground Spin States of Fe(II), Fe(III) and Fe(IV) Complexes. *Phys. Chem. Chem. Phys.* **2017**, *19*, 13049−13069.
(37) Phung, Q. M.; Feldt, M.; Harvey, J. N.; Pierloot, K. Toward Highly Accurate Spin State Energetics in First-Row Transition Metal Complexes: A Combined CASPT2/CC Approach. *J. Chem. Theory Comput.* **2018**, *14*, 2446−2455.
(38) Verma, P.; Varga, Z.; Truhlar, D. G. Hyper Open-Shell Excited Spin States of Transition-Metal Compounds: FeF_2, FeF_2···Ethane, and FeF_2···Ethylene. *J. Phys. Chem. A* **2018**, *122*, 2563−2579.
(39) Li Manni, G.; Kats, D.; Tew, D. P.; Alavi, A. Role of Valence and Semicore Electron Correlation on Spin Gaps in Fe(II)-Porphyrins. *J. Chem. Theory Comput.* **2019**, *15*, 1492−1497.
(40) Zhou, C.; Gagliardi, L.; Truhlar, D. G. Multiconfiguration Pair-Density Functional Theory for Iron Porphyrin with CAS, RAS, and DMRG Active Spaces. *J. Phys. Chem. A* **2019**, *123*, 3389−3394.
(41) Collman, J. P.; Hoard, J. L.; Kim, N.; Lang, G.; Reed, C. A. Synthesis, Stereochemistry, and Structure-Related Properties of $\alpha,\beta,\gamma,\delta$-Tetraphenylporphinatoiron(II). *J. Am. Chem. Soc.* **1975**, *97* (10), 2676−2681.
(42) Dolphin, D.; Sams, J. R.; Tsin, T. B.; Wong, K. L. Synthesis and Mossbauer Spectra of Octaethylporphyrin Ferrous Complexes. *J. Am. Chem. Soc.* **1976**, *98*, 6970−6975.
(43) Sligar, S. G. Coupling of Spin, Substrate, and Redox Equilibriums in Cytochrome P450. *Biochemistry* **1976**, *15*, 5399−5406.
(44) Lang, G.; Spartalian, K.; Reed, C. A.; Collman, J. P. Mössbauer Effect Study of the Magnetic Properties of S = 1 Ferrous Tetraphenylporphyrin. *J. Chem. Phys.* **1978**, *69*, 5424−5427.
(45) Boyd, P. D. W.; Buckingham, D. A.; McMeeking, R. F.; Mitra, S. Paramagnetic Anisotropy, Average Magnetic Susceptibility, and Electronic Structure of Intermediate-Spin S = 1 (5,10,15,20-Tetraphenylporphyrin)Iron(II). *Inorg. Chem.* **1979**, *18*, 3585−3591.
(46) Kitagawa, T.; Teraoka, J. The Resonance Raman Spectra of Intermediate-Spin Ferrous Porphyrin. *Chem. Phys. Lett.* **1979**, *63*, 443−446.
(47) Mispelter, J.; Momenteau, M.; Lhoste, J. M. Proton Magnetic Resonance Characterization of the Intermediate (S = 1) Spin State of Ferrous Porphyrins. *J. Chem. Phys.* **1980**, *72*, 1003−1012.
(48) Strauss, S. H.; Silver, M. E.; Long, K. M.; Thompson, R. G.; Hudgens, R. A.; Spartalian, K.; Ibers, J. A. Comparison of the Molecular and Electronic Structures of (2,3,7,8, 12,13,17,18-Octaethylporphyrinato)Iron(II) and (Trans-7,8-Dihydro-2,3,7,8,12,13,17,18-Octaethyl-Porphyrinato)Iron(II). *J. Am. Chem. Soc.* **1985**, *107*, 4207−4215.
(49) Munro, O. Q.; de Wet, M.; Pollak, H.; van Wyk, J.; Marques, H. M. Haempeptide Models for Haemoproteins Part 3: N-Acetylmicroperoxidase-8: EPR, Mössbauer and Magnetic Susceptibility Studies on an Iron(III) Porphyrin in Thermal Equilibrium between S= 3/2, 5/2 and S= 1/2 States. *J. Chem. Soc., Faraday Trans.* **1998**, *94*, 1743−1752.
(50) Kohn, W.; Sham, L. J. Self-Consistent Equations Including Exchange and Correlation Effects. *Phys. Rev.* **1965**, *140*, A1133−A1138.
(51) Kepp, K. P. Consistent Descriptions of Metal−Ligand Bonds and Spin-Crossover in Inorganic Chemistry. *Coord. Chem. Rev.* **2013**, *257*, 196−209.
(52) Caballol, R.; Castell, O.; Illas, F.; de P. R. Moreira, I.; Malrieu, J. P. Remarks on the Proper Use of the Broken Symmetry Approach to Magnetic Coupling. *J. Phys. Chem. A* **1997**, *101*, 7860−7866.
(53) González, L.; Escudero, D.; Serrano-Andrés, L. Progress and Challenges in the Calculation of Electronic Excited States. *ChemPhysChem* **2012**, *13*, 28−51.
(54) Jacob, C. R.; Reiher, M. Spin in Density-Functional Theory. *Int. J. Quantum Chem.* **2012**, *112*, 3661−3684.
(55) Reiher, M. Theoretical Study of the $Fe(Phen)_2(NCS)_2$ Spin-Crossover Complex with Reparametrized Density Functionals. *Inorg. Chem.* **2002**, *41*, 6928−6935.
(56) Deeth, R. J.; Fey, N. The Performance of Nonhybrid Density Functionals for Calculating the Structures and Spin States of Fe(II) and Fe(III) Complexes. *J. Comput. Chem.* **2004**, *25*, 1840−1848.
(57) Swart, M.; Groenhof, A. R.; Ehlers, A. W.; Lammertsma, K. Validation of Exchange-Correlation Functional for Spin States of Iron Complexes. *J. Phys. Chem. A* **2004**, *108*, 5479−5483.
(58) Ganzenmüller, G.; Berkaïne, N.; Fouqueau, A.; Casida, M. E.; Reiher, M. Comparison of Density Functionals for Differences between the High- ($^5T_{2g}$) and Low- ($^1A_{1g}$) Spin States of Iron(II) Compounds. IV. Results for the Ferrous Complexes [Fe(L)-('NHS_4')]. *J. Chem. Phys.* **2005**, *122*, 234321.
(59) Pierloot, K.; Vancoillie, S. Relative Energy of the High-($^5T_{2g}$) and Low-($^1A_{1g}$) Spin States of $[Fe(H_2O)_6]^{2+}$, $[Fe(NH_3)_6]^{2+}$, and $[Fe(Bpy)_3]^{2+}$: CASPT2 versus Density Functional Theory. *J. Chem. Phys.* **2006**, *125*, 124303.
(60) Radoń, M.; Broclawik, E.; Pierloot, K. Electronic Structure of Selected $\{FeNO\}^7$ Complexes in Heme and Non-Heme Architectures: A Density Functional and Multireference Ab Initio Study. *J. Phys. Chem. B* **2010**, *114*, 1518−1528.
(61) Gani, T. Z. H.; Kulik, H. J. Where Does the Density Localize? Convergent Behavior for Global Hybrids, Range Separation, and DFT +U. *J. Chem. Theory Comput.* **2016**, *12*, 5931−5945.
(62) Radoń, M. Revisiting the Role of Exact Exchange in DFT Spin-State Energetics of Transition Metal Complexes. *Phys. Chem. Chem. Phys.* **2014**, *16*, 14479−14488.
(63) Pinter, B.; Chankisjijev, A.; Geerlings, P.; Harvey, J. N.; De Proft, F. Conceptual Insights into DFT Spin-State Energetics of Octahedral Transition-Metal Complexes through a Density Difference Analysis. *Chem. - Eur. J.* **2018**, *24*, 5281−5292.
(64) Wilbraham, L.; Verma, P.; Truhlar, D. G.; Gagliardi, L.; Ciofini, I. Multiconfiguration Pair-Density Functional Theory Predicts Spin-State Ordering in Iron Complexes with the Same Accuracy as Complete Active Space Second-Order Perturbation Theory at a Significantly Reduced Computational Cost. *J. Phys. Chem. Lett.* **2017**, *8*, 2026−2030.
(65) Verma, P.; Truhlar, D. G. HLE16: A Local Kohn-Sham Gradient Approximation with Good Performance for Semiconductor Band Gaps and Molecular Excitation Energies. *J. Phys. Chem. Lett.* **2017**, *8*, 380−387.
(66) Verma, P.; Truhlar, D. G. HLE17: An Improved Local Exchange-Correlation Functional for Computing Semiconductor Band Gaps and Molecular Excitation Energies. *J. Phys. Chem. C* **2017**, *121*, 7144−7154.
(67) Raghavachari, K.; Trucks, G. W.; Pople, J. A.; Head-Gordon, M. A Fifth-Order Perturbation Comparison of Electron Correlation Theories. *Chem. Phys. Lett.* **1989**, *157*, 479−483.
(68) Feldt, M.; Phung, Q. M.; Pierloot, K.; Mata, R. A.; Harvey, J. N. Limits of Coupled-Cluster Calculations for Non-Heme Iron Complexes. *J. Chem. Theory Comput.* **2019**, *15*, 922−937.
(69) Roos, B. O. The Complete Active Space SCF Method in a Fock-matrix-based Super-CI Formulation. *Int. J. Quantum Chem.* **1980**, *18*, 175−189.
(70) Aquilante, F.; Autschbach, J.; Carlson, R. K.; Chibotaru, L. F.; Delcey, M. G.; De Vico, L.; Fdez. Galván, I.; Ferré, N.; Frutos, L. M.; Gagliardi, L.; et al. Molcas 8: New Capabilities for Multiconfigurational Quantum Chemical Calculations across the Periodic Table. *J. Comput. Chem.* **2016**, *37*, 506−541.

https://dx.doi.org/10.1021/acs.jpca.9b10772
J. Phys. Chem. A 2020, 124, 1187−1195

(71) Mizukami, W.; Kurashige, Y.; Yanai, T. More π Electrons Make a Difference: Emergence of Many Radicals on Graphene Nanoribbons Studied by *Ab Initio* DMRG Theory. *J. Chem. Theory Comput.* **2013**, *9*, 401−407.
(72) White, S. R. Density Matrix Formulation for Quantum Renormalization Groups. *Phys. Rev. Lett.* **1992**, *69*, 2863−2866.
(73) White, S. R. Density-Matrix Algorithms for Quantum Renormalization Groups. *Phys. Rev. B: Condens. Matter Mater. Phys.* **1993**, *48*, 10345−10356.
(74) White, S. R.; Martin, R. L. Ab Initio Quantum Chemistry Using the Density Matrix Renormalization Group. *J. Chem. Phys.* **1999**, *110*, 4127−4130.
(75) Schollwöck, U. The Density-Matrix Renormalization Group in the Age of Matrix Product States. *Ann. Phys. (Amsterdam, Neth.)* **2011**, *326*, 96−192.
(76) Knecht, S.; Hedegård, E. D.; Keller, S.; Kovyrshin, A.; Ma, Y.; Muolo, A.; Stein, C. J.; Reiher, M. New Approaches for Ab Initio Calculations of Molecules with Strong Electron Correlation. *Chimia* **2016**, *70*, 244−251.
(77) Malmqvist, P.-Å.; Rendell, A.; Roos, B. O. The Restricted Active Space Self-Consistent-Field Method, Implemented with a Split Graph Unitary Group Approach. *J. Phys. Chem.* **1990**, *94*, 5477−5482.
(78) Olsen, J.; Roos, B. O.; Jørgensen, P.; Jensen, H. J. A. Determinant Based Configuration Interaction Algorithms for Complete and Restricted Configuration Interaction Spaces. *J. Chem. Phys.* **1988**, *89*, 2185−2192.
(79) Valerrama, E.; Pradera, X.; Silanes, I.; Ugalde, J. M.; Boyd, R. J. Electron Correlation Studies by Means of Electron-Pair Density Functions. In *Reviews of Modern Quantum Chemistry*; Sen, K. D., Ed.; World Scientific: River Edge, New Jersey, 2002; pp 577−611.
(80) Andersson, K.; Malmqvist, P.-Å.; Roos, B. O.; Sadlej, A. J.; Wolinski, K. Second-Order Perturbation Theory with a CASSCF Reference Function. *J. Phys. Chem.* **1990**, *94*, 5483−5488.
(81) Andersson, K.; Malmqvist, P.-A.; Roos, B. O. Second-Order Perturbation Theory with a Complete Active Space Self-Consistent Field Reference Function. *J. Chem. Phys.* **1992**, *96*, 1218−1226.
(82) Pulay, P. A Perspective on the CASPT2 Method. *Int. J. Quantum Chem.* **2011**, *111*, 3273−3279.
(83) Hirao, K. Multireference Møller—Plesset Method. *Chem. Phys. Lett.* **1992**, *190*, 374−380.
(84) Malmqvist, P. Å.; Pierloot, K.; Shahi, A. R. M.; Cramer, C. J.; Gagliardi, L. The Restricted Active Space Followed by Second-Order Perturbation Theory Method: Theory and Application to the Study of CuO2 and Cu2O2 Systems. *J. Chem. Phys.* **2008**, *128*, 204109.
(85) Kurashige, Y.; Yanai, T. Second-Order Perturbation Theory with a Density Matrix Renormalization Group Self-Consistent Field Reference Function: Theory and Application to the Study of Chromium Dimer. *J. Chem. Phys.* **2011**, *135*, No. 094104.
(86) Sand, A. M.; Truhlar, D. G.; Gagliardi, L. Efficient Algorithm for Multiconfiguration Pair-Density Functional Theory with Application to the Heterolytic Dissociation Energy of Ferrocene. *J. Chem. Phys.* **2017**, *146*, No. 034101.
(87) Sand, A. M.; Truhlar, D. G.; Gagliardi, L. Erratum: "Efficient Algorithm for Multiconfiguration Pair-Density Functional Theory with Application to the Heterolytic Dissociation Energy of Ferrocene" [J. Chem. Phys. 146, 034101 (2017)]. *J. Chem. Phys.* **2017**, *146*, 189901.
(88) Iron, M. A.; Oren, M.; Martin, J. M. L. Alkali and Alkaline Earth Metal Compounds: Core—Valence Basis Sets and Importance of Subvalence Correlation. *Mol. Phys.* **2003**, *101*, 1345−1361.
(89) Bistoni, G.; Riplinger, C.; Minenkov, Y.; Cavallo, L.; Auer, A. A.; Neese, F. Treating Subvalence Correlation Effects in Domain Based Pair Natural Orbital Coupled Cluster Calculations: An Out-of-the-Box Approach. *J. Chem. Theory Comput.* **2017**, *13*, 3220−3227.
(90) Solomonik, V. G.; Smirnov, A. N. Toward Chemical Accuracy in Ab Initio Thermochemistry and Spectroscopy of Lanthanide Compounds: Assessing Core-Valence Correlation, Second-Order Spin-Orbit Coupling, and Higher Order Effects in Lanthanide Diatomics. *J. Chem. Theory Comput.* **2017**, *13*, 5240−5254.
(91) Purvis, G. D.; Bartlett, R. J. A Full Coupled-Cluster Singles and Doubles Model: The Inclusion of Disconnected Triples. *J. Chem. Phys.* **1982**, *76*, 1910−1918.
(92) Radoń, M. Benchmarking Quantum Chemistry Methods for Spin-State Energetics of Iron Complexes against Quantitative Experimental Data. *Phys. Chem. Chem. Phys.* **2019**, *21*, 4854−4870.
(93) Li Manni, G.; Carlson, R. K.; Luo, S.; Ma, D.; Olsen, J.; Truhlar, D. G.; Gagliardi, L. Multiconfiguration Pair-Density Functional Theory. *J. Chem. Theory Comput.* **2014**, *10*, 3669−3680.
(94) Gagliardi, L.; Truhlar, D. G.; Li Manni, G.; Carlson, R. K.; Hoyer, C. E.; Bao, J. L. Multiconfiguration Pair-Density Functional Theory: A New Way To Treat Strongly Correlated Systems. *Acc. Chem. Res.* **2017**, *50*, 66−73.
(95) Stoneburner, S. J.; Truhlar, D. G.; Gagliardi, L. MC-PDFT Can Calculate Singlet-Triplet Splittings of Organic Diradicals. *J. Chem. Phys.* **2018**, *148*, No. 064108.
(96) Carlson, R. K.; Li Manni, G.; Sonnenberger, A. L.; Truhlar, D. G.; Gagliardi, L. Multiconfiguration Pair-Density Functional Theory: Barrier Heights and Main Group and Transition Metal Energetics. *J. Chem. Theory Comput.* **2015**, *11*, 82−90.
(97) Carlson, R. K.; Truhlar, D. G.; Gagliardi, L. Multiconfiguration Pair-Density Functional Theory: A Fully Translated Gradient Approximation and Its Performance for Transition Metal Dimers and the Spectroscopy of $Re_2Cl_8^{2-}$. *J. Chem. Theory Comput.* **2015**, *11*, 4077−4085.
(98) Carlson, R. K.; Li Manni, G.; Sonnenberger, A. L.; Truhlar, D. G.; Gagliardi, L. Correction to Multiconfiguration Pair-Density Functional Theory: Barrier Heights and Main Group and Transition Metal Energetics. *J. Chem. Theory Comput.* **2016**, *12*, 457.
(99) Bao, J. L.; Odoh, S. O.; Gagliardi, L.; Truhlar, D. G. Predicting Bond Dissociation Energies of Transition-Metal Compounds by Multiconfiguration Pair-Density Functional Theory and Second-Order Perturbation Theory Based on Correlated Participating Orbitals and Separated Pairs. *J. Chem. Theory Comput.* **2017**, *13*, 616−626.
(100) Sharkas, K.; Gagliardi, L.; Truhlar, D. G. Multiconfiguration Pair-Density Functional Theory and Complete Active Space Second Order Perturbation Theory. Bond Dissociation Energies of FeC, NiC, FeS, NiS, FeSe, and NiSe. *J. Phys. Chem. A* **2017**, *121*, 9392−9400.
(101) Presti, D.; Truhlar, D. G.; Gagliardi, L. Intramolecular Charge Transfer and Local Excitation in Organic Fluorescent Photoredox Catalysts Explained by RASCI-PDFT. *J. Phys. Chem. C* **2018**, *122*, 12061−12070.
(102) Sharma, P.; Truhlar, D. G.; Gagliardi, L. Multiconfiguration Pair-Density Functional Theory Investigation of the Electronic Spectrum of MnO_4^-. *J. Chem. Phys.* **2018**, *148*, 124305.
(103) Perdew, J. P.; Burke, K.; Ernzerhof, M. Generalized Gradient Approximation Made Simple. *Phys. Rev. Lett.* **1996**, *77*, 3865−3868.
(104) Sharma, P.; Bernales, V.; Truhlar, D. G.; Gagliardi, L. Valence ππ* Excitations in Benzene Studied by Multiconfiguration Pair-Density Functional Theory. *J. Phys. Chem. Lett.* **2019**, *10*, 75−81.
(105) Presti, D.; Kadlec, J.; Truhlar, D. G.; Gagliardi, L. Scaling Exchange and Correlation in the On-Top Functional of Multi-Configuration Pair-Density Functional Theory: Electronic Excitation Energies and Bond Energies. *Theor. Chem. Acc.* **2020**, *139*, 1.
(106) Chen, H.; Lai, W.; Shaik, S. Exchange-Enhanced H-Abstraction Reactivity of High-Valent Nonheme Iron(IV)-Oxo from Coupled Cluster and Density Functional Theories. *J. Phys. Chem. Lett.* **2010**, *1*, 1533−1540.
(107) Kirkland, J. K.; Khan, S. N.; Casale, B.; Miliordos, E.; Vogiatzis, K. D. Ligand Field Effects on the Ground and Excited States of Reactive FeO^{2+} Species. *Phys. Chem. Chem. Phys.* **2018**, *20*, 28786−28795.
(108) Hoyer, C. E.; Ghosh, S.; Truhlar, D. G.; Gagliardi, L. Multiconfiguration Pair-Density Functional Theory Is as Accurate as CASPT2 for Electronic Excitation. *J. Phys. Chem. Lett.* **2016**, *7*, 586−591.
(109) Zhang, Y.; Yang, W. Comment on "Generalized Gradient Approximation Made Simple. *Phys. Rev. Lett.* **1998**, *80*, 890−890.

https://dx.doi.org/10.1021/acs.jpca.9b10772
J. Phys. Chem. A 2020, 124, 1187−1195

(110) Vosko, S. H.; Wilk, L.; Nusair, M. Accurate Spin-Dependent Electron Liquid Correlation Energies for Local Spin Density Calculations: A Critical Analysis. *Can. J. Phys.* **1980**, *58*, 1200−1211.
(111) Becke, A. D. Density-Functional Exchange-Energy Approximation with Correct Asymptotic Behavior. *Phys. Rev. A: At., Mol., Opt. Phys.* **1988**, *38*, 3098−3100.
(112) Ghigo, G.; Roos, B. O.; Malmqvist, P.-Å. A Modified Definition of the Zeroth-Order Hamiltonian in Multiconfigurational Perturbation Theory (CASPT2). *Chem. Phys. Lett.* **2004**, *396*, 142−149.
(113) Forsberg, N.; Malmqvist, P.-Å. Multiconfiguration Perturbation Theory with Imaginary Level Shift. *Chem. Phys. Lett.* **1997**, *274*, 196−204.
(114) Roos, B. O. The Complete Active Space Self-Consistent Field Method and Its Applications in Electronic Structure Calculations. In *Advances in Chemical Physics: Ab Initio Methods in Quantum Chemistry, Part II*; Lawley, K. P., Ed.; Wiley: New York, New York, 1987; Vol. *69*, pp 399−445.
(115) Balabanov, N. B.; Peterson, K. A. Systematically Convergent Basis Sets for Transition Metals. I. All-Electron Correlation Consistent Basis Sets for the 3*d* Elements Sc-Zn. *J. Chem. Phys.* **2005**, *123*, No. 064107.
(116) Dunning, T. H. Gaussian Basis Sets for Use in Correlated Molecular Calculations. I. The Atoms Boron through Neon and Hydrogen. *J. Chem. Phys.* **1989**, *90*, 1007−1023.
(117) Kendall, R. A.; Dunning, T. H., Jr.; Harrison, R. J. Electron Affinities of the First-Row Atoms Revisited. Systematic Basis Sets and Wave Functions. *J. Chem. Phys.* **1992**, *96*, 6796−6806.
(118) Woon, D. E.; Dunning, T. H. Gaussian Basis Sets for Use in Correlated Molecular Calculations. III. The Atoms Aluminum through Argon. *J. Chem. Phys.* **1993**, *98*, 1358−1371.
(119) Aquilante, F.; Bondo Pedersen, T.; Sánchez de Merás, A.; Koch, H. Fast Noniterative Orbital Localization for Large Molecules. *J. Chem. Phys.* **2006**, *125*, 174101.
(120) Hess, B. A. Relativistic Electronic-Structure Calculations Employing a Two-Component No-Pair Formalism with External-Field Projection Operators. *Phys. Rev. A: At., Mol., Opt. Phys.* **1986**, *33*, 3742−3748.
(121) Reiher, M.; Wolf, A. Exact Decoupling of the Dirac Hamiltonian. I. General Theory. *J. Chem. Phys.* **2004**, *121*, 2037−2047.
(122) Reiher, M.; Wolf, A. Exact Decoupling of the Dirac Hamlltonian. II. The Generalized Douglas-Kroll-Hess Transformation up to Arbitrary Order. *J. Chem. Phys.* **2004**, *121*, 10945−10956.
(123) Howes, B. D.; Feis, A.; Indiani, C.; Marzocchi, M. P.; Smulevich, G. Formation of Two Types of Low-Spin Heme in Horseradish Peroxidase Isoenzyme A2 at Low Temperature. *JBIC, J. Biol. Inorg. Chem.* **2000**, *5*, 227−235.
(124) Decker, A.; Rohde, J.-U.; Klinker, E. J.; Wong, S. D.; Que, L.; Solomon, E. I. Spectroscopic and Quantum Chemical Studies on Low-Spin Fe^{IV}=O Complexes: Fe-O Bonding and Its Contributions to Reactivity. *J. Am. Chem. Soc.* **2007**, *129*, 15983−15996.
(125) Sharma, P.; Bernales, V.; Knecht, S.; Truhlar, D. G.; Gagliardi, L. Density Matrix Renormalization Group Pair-Density Functional Theory (DMRG-PDFT): Singlet-Triplet Gaps in Polyacenes and Polyacetylenes. *Chem. Sci.* **2019**, *10*, 1716−1723.

https://dx.doi.org/10.1021/acs.jpca.9b10772
J. Phys. Chem. A 2020, 124, 1187−1195